FINITE DIFFERENCE ANALYSES OF SCHUMANN RESONANCE AND RECONSTRUCTION OF LIGHTNING DISTRIBUTION

Yoshiaki Ando and Masashi Hayakawa

The University of Electro-Communications

1-5-1 Chofugaoka, Chofu-shi, Tokyo, 182-8585, Japan

E-mail: ando@whistler.ee.uec.ac.jp

1 Introduction

The objective of our study is to establish a method to draw the world map of lightning activity by observing Schumann resonance spectra at a few ground observatories. Schumann resonances are resonant phenomena in the extremely low frequency (ELF) band in the cavity which consists of a global spherical shell between the earth's surface and the ionosphere [1, 2], and the resonant frequencies are about 7, 14, 20 Hz, and so on, which correspond to the first, second, third resonant frequencies, respectively. Schumann resonances are observable all over the world, and the spectra depend mostly on distance between the source lightning and the observation point. In other words, the measured ELF spectra have the information on the sources and the propagation paths. The use of Schumann resonance for the lightning world map takes much less costs than the use of satellites in respects of observation and maintenance.

In this paper, we calculate observable Schumann spectra by the frequency-domain finite difference (FDFD) method, which makes it possible to introduce realistic profiles, and we utilize the International Reference Ionosphere 2000 (IRI 2000)[3] and the mass spectrometer incoherent scatter (NRLMSISE-00) model[4], as widely accepted electron and neutral density profile models. The reconstruction of the lightning source distribution from the resonant ELF spectra was developed by Shvets[5]. In this paper, we adopt his method entirely, but with the results calculated by the FDFD method, and apply the approach presented here to the observed data in order to identify lightning activity regions.

2 Finite difference method

2.1 Derivation of finite difference equations

The geometry and the coordinates for our analysis are taken as shown in Fig.1. The analysis region lies between the inner perfect conductor with the radius r_i, corresponding to the earth, and the outer one with the radius r_o. It will be demonstrated later from numerical results that the absorbing boundaries are not necessary if we keep sufficient altitude in the analysis region, because electromagnetic fields in the ELF band under consideration are reflected and dissipated enough by the ionosphere, and we can truncate the analysis region, that is, put the outer conductor at the altitude of about 130km. It is assumed that the problem is symmetric over the azimuth, or $\partial/\partial\varphi = 0$. The analysis region is discretized by Δr and $\Delta\theta$ in the r- and θ-coordinates, respectively. As a result, points in the discretized coordinates are represented by $(r, \theta) = (r_i + \{i-1\}\Delta r, \{j-1\}\Delta\theta) \equiv (i, j)$, where i runs from 1 to N with the definition $r_o = r_i + N\Delta r$, and j does from 1 to M with $M\Delta\theta = \pi$. The current source with the length Δl and the intensity I is located near the surface of the inner conductor, and directed radially. In the present configuration, only TE mode with respect to φ-direction is excited; that is, E_r, E_θ, and H_φ are nonzero components which are assigned on staggered points of cells as Yee's algorithm[6]:
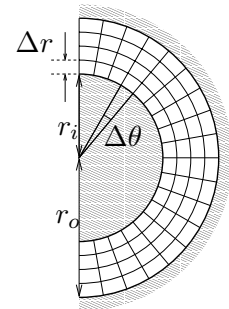
$$E_r(\{i+\tfrac{1}{2}\}\Delta r, j\,\Delta\theta), \quad E_\theta(i\,\Delta r, \{j+\tfrac{1}{2}\}\Delta\theta), \quad H_\varphi(\{i+\tfrac{1}{2}\}\Delta r, \{j+\tfrac{1}{2}\}\Delta\theta) \quad (1)$$

The finite difference equations are given in terms of the magnetic field:

$$a_1 H_\varphi(i + \tfrac{3}{2}, j + \tfrac{1}{2}) + a_2 H_\varphi(i - \tfrac{1}{2}, j + \tfrac{1}{2}) + a_3 H_\varphi(i + \tfrac{1}{2}, j + \tfrac{3}{2})$$
$$+ a_4 H_\varphi(i + \tfrac{1}{2}, j - \tfrac{1}{2}) + a_0 H_\varphi(i + \tfrac{1}{2}, j + \tfrac{1}{2}) = b. \quad (2)$$

Figure 1: Analysis model

The coefficients are given by

$$a_1 = -\frac{(1 - \delta_{N,i})\,R(i + \tfrac{3}{2})}{\epsilon_r(i+1, j+\tfrac{1}{2})\,R(i+\tfrac{1}{2})}, \quad a_2 = -\frac{(1 - \delta_{1,i})R(i-\tfrac{1}{2})}{\epsilon_r(i, j+\tfrac{1}{2})\,R(i+\tfrac{1}{2})},$$

$$a_3 = -\frac{(1 - \delta_{1,M})S(j + \frac{3}{2})(\Delta r)^2}{\epsilon_r(i + \frac{1}{2}, j + 1)R(i + \frac{1}{2})^2(\Delta\theta)^2 S(j + 1)}, \quad a_4 = -\frac{(1 - \delta_{1,j})S(j - \frac{1}{2})(\Delta r)^2}{\epsilon_r(i + \frac{1}{2}, j)R(i + \frac{1}{2})^2(\Delta\theta)^2 S(j)},$$

$$a_0 = -k_0^2(\Delta r)^2 + \left[\frac{(1 - \delta_{N,i})}{\epsilon_r(i + 1, j + \frac{1}{2})} + \frac{(1 - \delta_{1,i})}{\epsilon_r(i, j + \frac{1}{2})}\right] + \frac{S(j + \frac{1}{2})(\Delta r)^2}{\{R(i + \frac{1}{2})\Delta\theta\}^2}\left[\frac{A_{j,1}}{\epsilon_r(i + \frac{1}{2}, j)} + \frac{A_{j,M}}{\epsilon_r(i + \frac{1}{2}, j + 1)}\right],$$

$$b^{(1)} = \frac{4I\,\Delta l\,\Delta r\,\delta_{i,1}\,\delta_{j,1}}{\epsilon(i + \frac{1}{2}, 1)\pi\{R(i + \frac{1}{2})\,\Delta\theta\}^3}$$

where k_0, $\delta_{m,n}$, $R(i)$, and $S(j)$ are the wavenumber of light in vacuum, the Kronecker's delta, $R(i) = r_i + (i - 1)\Delta r$, and $S(j) = \sin\{(j - 1)\Delta\theta\}$, respectively, and

$$A_{j,1} = \begin{cases} \dfrac{1}{S(j)}, & (j \neq 1) \\ \dfrac{4}{S(j + \frac{1}{2})}, & (j = 1) \end{cases} \qquad A_{M,1} = \begin{cases} \dfrac{1}{S(j + 1)}, & (j \neq M) \\ \dfrac{4}{S(j + \frac{1}{2})}. & (j = M) \end{cases}$$

We will consider the dielectric constant, $\epsilon_r(i, j)$, later. The electric field is given from the obtained magnetic field by the straightforward finite difference procedure.

2.2 Conductivity profile

The cavity of Schumann resonances is dissipative, and the losses are due to collision among charged and neutral particles, and are characterized by the conductivity. In the lower atmosphere, the contribution to the conductivity is mainly by ions. The conductivity profile in these regions is well modeled by

$$\frac{1}{\sigma(z)} = \sum_{i=1}^{3} A_e e^{-B_i z}, \quad \text{where} \quad \left(\frac{A_i}{10^{12}\Omega\text{m}}, \frac{B_i}{\text{km}^{-1}}\right) = (46.9, 4.527)_1, (22.2, 0.375)_2, (5.9, 0.121)_3. \tag{3}$$

We use this model at the altitude lower than 60 km. Above there, the electron has the dominant contribution to the conductivity. In this region, the medium is characterized directly by the dielectric constant: $\epsilon_r = 1 - \omega_{pe}^2/\{\omega - j(\nu_{en} + \nu_{ei})\}\omega$, where ω_{pe}, ω, ν_{en} and ν_{ei} are the electron plasma frequency, the angular wave frequency, and the collision frequency between electrons and neutral particles, and between electrons and ions, respectively. ν_{en} and ν_{ei} are given by

$$\nu_{en} = \{4.6N_{N_2}R_e^{0.95} + 4.3N_{O_2}R_e^{0.79} + 1.5N_O R_e^{0.85}\} \times 10^{-15}\ \text{m}^3\text{s}^{-1}, \tag{4}$$

$$\nu_{ei} = (1.84 \times 10^{-6}\text{s}^{-1}\text{m}^3\text{K}^{3/2})\{16.33 + 0.5\ln(T_e^3/N_e)\}N_e T_e^{-3/2}, \tag{5}$$

where N_{N_2}, N_{O_2}, and N_O are the concentration (in m^{-3}) of N_2, O_2, and N_O. R_e is $T_e/(300\text{ K})$, and T_e is temperature of electrons in K. The concentrations and temperatures of electrons, ions, and neutrals are given by the IRI model[3], and the NRLMSISE-00 model[4]. The temperature of electrons is assumed to be equal to the one of neutrals in the D-region of the ionosphere.

The electron density profiles depend on latitude, longitude, and time. But we assume that the profile is uniform all over the region, and the profile at the observation point is used. It was examined that the difference of those profiles under the usual condition did not make significant effects on numerical results.

2.3 Numerical results

Some numerical examples are demonstrated in this section. The observation point is assumed to be located at Moshiri, Hokkaido, Japan (44° 20′N 142° 15′E) where we have actually been measuring the Schumann spectra for the last 5 years. The parameters for calculation are chosen as follows: $r_i = 6370$ [km], $\Delta r = 5$ [km], $r_i\,\Delta\theta = 10.0$ [km], and $r_o = 6370 + 130$ [km]. Relatively finer discretization is necessary for the radial direction because of modeling of the electron profile.

Fig.2 shows the amplitude of calculated magnetic field. The source is located on the top surface of the earth in this figure. For visualization, we magnify the altitude of the analysis region 20 times. The

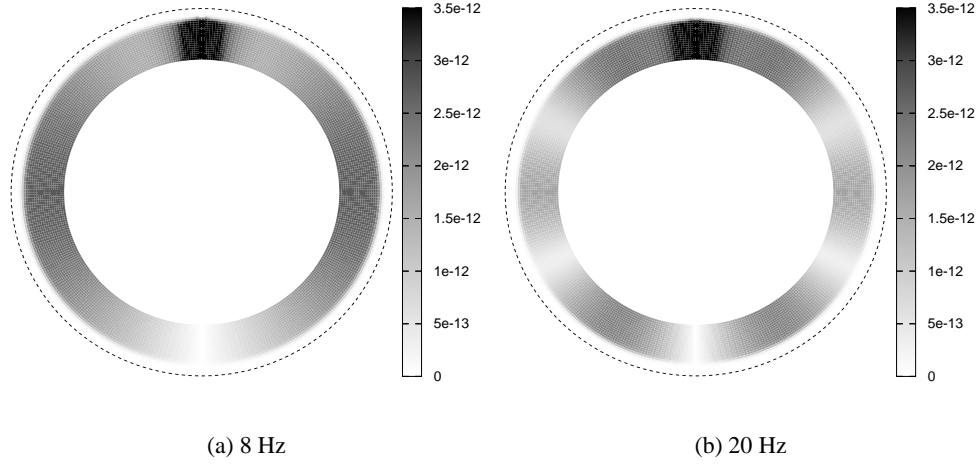(a) 8 Hz   (b) 20 Hz

Figure 2: Numerical result of distribution of magnetic field intensity

frequencies used in this calculation are 8 Hz and 20 Hz which almost correspond to the first and the third resonant frequencies in this resonator, as observed from Fig. 2. It is evident from this figure that the absorbing boundary condition is not necessary in this analysis because the fields decay rapidly at the altitude of about 80 km, and the reflection at the outer boundary does not affect numerical results.

Measurable field is the one on the earth's surface. Thus, Schumann resonant spectrum is obtained by collecting the surface field at the observation point with sweeping frequencies in the computation.

3 Reconstruction of lightning distribution

3.1 Inverse problem

Our problem is to reconstruct the lightning distribution ranging over the observation point through the antipodal point on the earth. This inverse problem was formulated and already well examined by Shvets[5]. Here we follow his method except the set of basis functions, and, thus we describe it briefly.

We divide the region (20Mm) by N and let the response of magnetic fields from the j-th region lightning be $h_j(f_i)$, where f_i's are discretized frequencies, and we define $|h_j(f_i)|^2 \equiv A_{ij}$. The square of a measured response, $b(f_i)$, is assumed to be a linear combination of A_{ij} with coefficients x_j's which correspond to a mean intensity of lightning over the j-th region. Thus, $\boldsymbol{b} = \mathbf{A} \cdot \boldsymbol{x}$, where the i-th components of $\boldsymbol{b}$ and $\boldsymbol{x}$ are $b(f_i)$ and x_i, respectively.

In order to find the solution, introducing Tikhonov's regularization yields the smoothing functional, $\Pi(\boldsymbol{x}) = \|\mathbf{A} \cdot \boldsymbol{x} - \boldsymbol{b}\| + \alpha\|\boldsymbol{x}\|^2$, and the solution is given from the condition that the gradient, $\mathbf{A}^T \cdot (\mathbf{A} \cdot \boldsymbol{x} - \boldsymbol{b}) + \alpha\boldsymbol{x}$, vanishes in the sense of the nonnegative least square[5].

3.2 Application to measured data

The reconstruction method is applied to the real data which were measured at Moshiri(44° 20′N 142° 15′E). The measurement setup is described in the Ref.[7]. The parameters to obtain the inverse problem solutions are : $M = 144$, $N = 40$, $\alpha = 4 \times 10^{-16}$, $\Delta r = 5$ [km], and $r_i \Delta\theta = 10.0$ [km]. The calculated result is shown in Figs. 3 as a grayscale map of daily variation on March 1, 1999. It is observed that there are two active regions mainly, one is about 10 Mm from the observation point and another is about 12 Mm. The reconstructed Schumann spectrum is plotted in Fig.4 by the solid curve, with the measured spectrum by dots. It is noted that the $1/f^n$ ($n = 0, 1, 2$) noises are included in the reconstruction function sets. We can see from Fig.4 that in this frequency range the measured spectrum is recovered well.

In order to verify the validity of the present method, we compare our results with the measured data by the Lightning Imaging Sensor (LIS) [8] at 1:00UT data as shown in Fig.5. The solid line is the approximate projection of the TRMM satellite orbit on the earth's surface from 00:35UT to 02:08UT, and the detected lightnings from 00:59UT to 01:13UT are indicated by stars. In this period the lightnings in Africa and the Middle East were observed. Three lightning active regions are expected from our result,
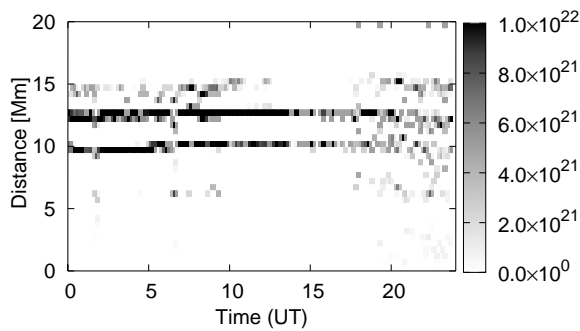
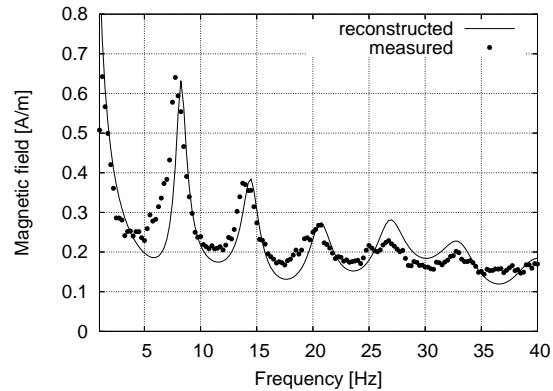Figure 3: Daily variation of reconstructed lightning activity on March 1, 1999.

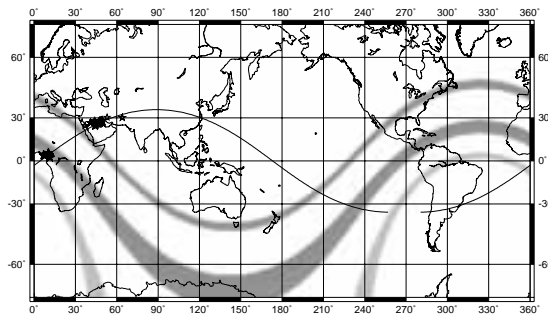

Figure 4: Reconstructed spectrum and measured data.

Figure 5: Reconstructed lightning activity region and LIS observation data.

which are shown in Fig.5 by gray bands. Two of them show good agreement with the LIS observation, one is from the middle Africa and another is from the Middle Eastern region, but the farest one from the observation point is not identified. Our result may expect that there is a lightning active region in the Southern Africa or South America.

4 Conclusion

The finite difference method for Schumann resonance analysis has been developed in the simplified uniform cavity. The atmospheric and ionospheric parameters are derived from IRI 2000, and NRLMSISE-00 models, to calculate realistic Schumann resonance spectra. The identification of lightning activity distribution has been successful, and the distribution is obtained with respect to distance from the observation point. We have applied the present method to the observed data at Hokkaido, Japan, and compared the result with the LIS data. Both the data show excellent agreement.

References

[1] W. O. Schumann, Z.Naturforschaftung, vol.72, pp.250-252, 1952.

[2] A. P. Nickolaenko and M. Hayakawa, Resonances in the Earth-Ionosphere Cavity, Kluwer, Dordrecht, Netherlands, 2002.

[3] D. Bilitza, Radio Sci., vol.36, no.2, pp.261-275, 2001.

[4] J. M. Picone, et al., J. Geophys. Res., vol.107, no.A12, doi:10.1029/2002JA009430, 2002.

[5] A. V. Shvets, J. Atmos. Solar-Terr. Phys., vol.63, pp.1061-1074, 2001.

[6] K. Yee, IEEE Trans. Antennas and Propagation, vol.14, no.3, pp.302-307, 1966.

[7] Y. Hobara, et al., J. Atmos. Electr., vol.20, no.2, pp.99-109, 2000.

[8] H. Christian, et al., Proc. 11th Int'l Conf. on Atmos. Electr., pp.746-749, Guntersville, Alabama, June 7-11, 1999.